Triboelectrification between Smooth Metal Surfaces Coated with Self-Assembled Monolayers (SAMs)†

Mustafa Akbulut,‡ Anna R. Godfrey Alig,‡ and Jacob Israelachvili*,§

Departments of Chemical Engineering and Materials, and the Materials Research Laboratory, University of California, Santa Barbara

Received: May 23, 2006; In Final Form: September 29, 2006

Using a modified surface forces apparatus, we have simultaneously measured the friction and triboelectrification between both similar and dissimilar molecularly smooth hexadecanethiol-coated metal surfaces on mica substrates. On shearing dissimilar surfaces, the tribocurrent increases dramatically as the load or pressure is increased, with large fluctuations about the mean. Neither charge transfer nor fluctuations are observed when the symmetric surfaces are sheared against each other. We also find that the type of friction, i.e., stick−slip or smooth sliding, the load and friction force, the sliding distance, and recent previous history have additional fine influences on the triboelectrification. Our results suggest that frictional dissipation induces electron−hole formation and charge transfer between two shearing surfaces due to molecular-level roughness and defects and local dielectric constant changes, giving rise to the observed tribocurrents.

Introduction

The existence of triboelectrification, or shear-induced charge transfer, has been known for a long time, although the basic mechanism is still not fully understood. When two surfaces are brought into *static* contact, charge is transferred due to the difference in their work functions.[1−3] If the surfaces are also sheared, under "ideal" conditions (wearless sliding of mathematically flat surfaces), the charge transfer should be the same as during static contact. In real, nonideal, systems (e.g., rough or coated surfaces), shear or friction-induced changes in the nanoscale structure and other physicochemical properties of the surfaces are expected to affect the charge transfer.

Understanding triboelectrification is fundamentally and practically important: (1) Charge transfer can determine tribological properties such as the friction force itself.[4,5] (2) Shear-induced charge transfer can result in sparking and stimulate chemical reactions which can cause corrosion, fire, and damage.[6] (3) The performance of small moving electronic devices such as microelectromechanical systems (MEMS) is particularly prone to failure caused by triboelectric effects.

Previous studies have tried to gain insight into the mechanism of triboelectrification by investigating the correlation between the charge transferred and the friction parameters such as the load, adhesion, sliding velocity, and friction force and type between dissimilar (asymmetric) surfaces.[7−15] These studies suggested that temperature gradients, differential stresses and strains, material transfer, and stochastic bond formation and breakage between the shearing surfaces cause charge transfer during sliding. None of these studies investigated friction-induced transient charge-transfer processes between two shearing surfaces with equal or equalized work potentials.

We have investigated shear-induced currents between various combinations of the molecularly smooth metal surfaces of Au, Ag, and Ti, each coated with a self-assembled monolayer (SAM) of hexadecanethiol. We selected the SAMs due to their ease of deposition, producing good-quality monolayers on these metals, and to prevent the metals from cold-welding. Metals were also chosen for their different work functions: $W_{Au} = 5.1 \pm 0.1$ eV, $W_{Ag} = 4.0 \pm 0.15$ eV, and $W_{Ti} = 4.33 \pm 0.1$ eV.[16−18] We used a surface forces apparatus to carry out these measurements, where two surfaces are connected through a picoammeter to measure the current generated during sliding. This setup provides us with two metal surfaces with equal Fermi levels (equalized work potentials) from the start (since the two surfaces are connected through a low-resistance picoammeter). Thus, we can eliminate the effect of work function differences and directly investigate nonideal charge-transfer behavior induced by frictional sliding.

Experimental Methods

Figure 1 shows schematics of the steps involved in the surface preparation for these experiments. First, atomically smooth sheets of back-silvered muscovite mica (S&J Trading, Glen Oaks, NY) were glued to silica disks with UV-cured glue (Norland Optical Adhesive 61). Metal films, approximately 80 Å thick, were deposited on the mica surfaces by e-beam deposition where the surfaces were cleaned in an ozone-cleaner for 3 min before deposition. The metal films were of Ag, Ti, or Au, where each Au film was deposited over a 16−18 Å layer of Cr for good adhesion and smoothness. After the metal deposition, the surfaces were stored in a desiccator until used. Prior to use, very thin, shielded, flexible wires (Cooner wire, AS631) were connected to the upper metal film of each surface using conducting epoxy (Circuitworks, CW2400). After the glue was thoroughly cured, the surfaces were placed, metal sides up, in a solution of 1 mM of 1-hexadecanethiol, $C_{16}S$ (Aldrich, purity 92%) in ethanol for 10 min. Then, the $C_{16}S$ monolayer was thoroughly dried for 30−60 min, and the conducting epoxy bond was strengthened and insulated by coating it with a thin layer of cyanoacrylate glue.

† Part of the special issue "Charles M. Knobler Festschrift".
‡ Department of Chemical Engineering.
§ Departments of Chemical Engineering and Materials, and the Materials Research Laboratory.

10.1021/jp063161j CCC: $33.50
Published on Web 10/17/2006

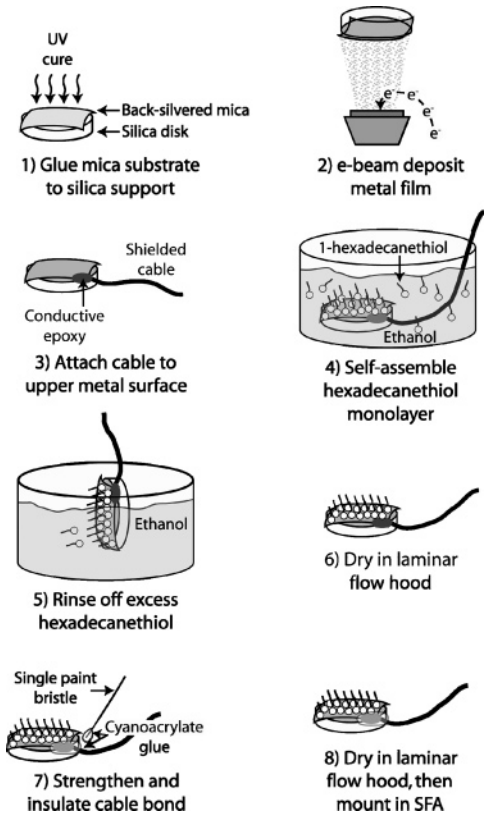

Figure 1. Schematic of the eight steps involved in preparing the surfaces.

Two disks were then mounted in the SFA chamber in a crossed-cylinder configuration as shown in Figure 2. It was important to arrange the disks such that the protruding conducting epoxy bonds did not interfere with each other (touch) or with the opposite surfaces during sliding. The shielded wires were connected to an electrical feed-through in the SFA. Phosphorus pentoxide (P_2O_5) was placed in the sealed SFA chamber, previously purged and then filled with dry nitrogen gas, to remove water from the air. The metal SFA chamber conveniently acts as a Faraday cage to help eliminate external noise. The wires were then connected to a Keithley picoammeter (model #6485) through low-noise BNC cables. The bottom surface is grounded to an electron sink. The picoammeter is a feedback picoammeter, which has certain limitations: it requires a voltage burden of 200 μV to operate. This determines the accuracy of the current and charge-transfer measurements, which depended on the contact resistance, and consequently on the pressures and different surfaces tested. Shear measurements were carried out by using either a motor-driven stage or a piezoelectric bimorph slider.[19] However, only the motor drive was used during the triboelectrification measurements to prevent possible electronic interference.

The surfaces were imaged by multiple beam interferometry using fringes of equal chromatic order (FECO), which allowed measurement of the thickness and uniformity of the monolayers (to $\sim$2 Å)[47] and the molecular contact area (lateral distance resolution $\sim$1 μm) as illustrated in Figure 2.[20]

AFM imaging of the SAM surfaces indicates that the surfaces have a root-mean-square (rms) roughness of less than 2 Å, allowing us to eliminate microscopic, but not nanoscopic, defects, "pinholes", or roughness in our study. No damage during or after sliding was observed either by the FECO or AFM imaging, except where mentioned (as in Figure 6).

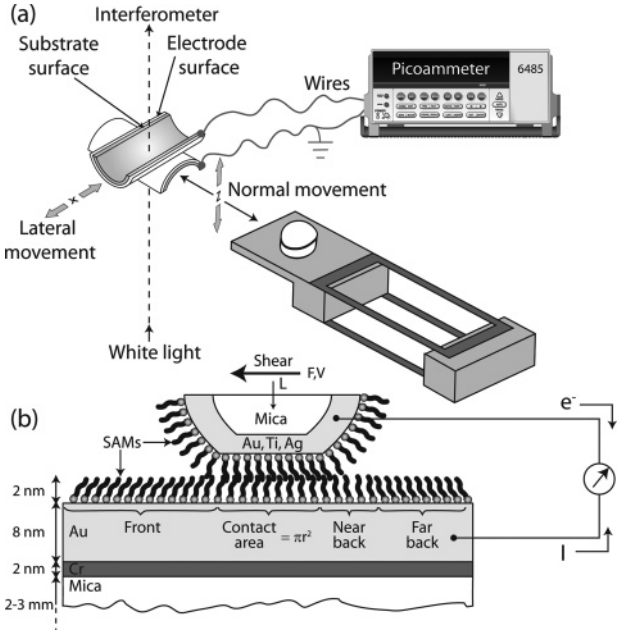

Figure 2. Schematics of (a) the experimental setup and (b) the contact geometry during sliding the top and bottom molecules in the $C_{16}S$ monolayers. The monolayers experience different forces and histories at different locations and times and also after reversing the sliding direction when the "front" and "back" parts interchange. Contact diameters were 40−250 μm, corresponding to contact areas of $\pi r^2 = (1-50) \times 10^3$ μm^2, loads applied were 0−200 mN, mean applied pressures[46] (load/contact area) were $P = L/\pi r^2 = \sim$0−8 MPa, motor drive velocities were $V = 0.2-2.0$ μm/s when the mechanized motor drive was used, sliding times (before reversals) were 10−100 s, and sliding distances (before reversals) were 10−90 μm, i.e., about 35% of the contact diameter, $2r$. The horizontal double-cantilever springs in (a) are for measuring the normal forces, L; vertical springs (not shown) are used to measure the friction forces, F.

TABLE 1: Water Contact Angles of 1-hexadecanethiol SAMs on Different Metal Surfaces

	static θ_S	advancing θ_A	receding θ_R	hysteresis $\Delta\theta = (\theta_A - \theta_R)$
Au	107.0 ± 2.4	105.0 ± 2.9	98.1 ± 2.6	6.9 ± 3.9
Ag	108.4 ± 2.2	107.3 ± 1.9	98.2 ± 2.2	9.1 ± 2.9
Ti	93.8 ± 2.6	93.8 ± 4.2	69.0 ± 4.8	24.8 ± 6.3

The SFA was also used to measure the adhesion or "pull-off" forces L_{ad} needed to separate/detach the surfaces from adhesive contact. These were determined from the measured jump-out distances multiplied by the stiffness (spring constant) K of the normal force-measuring spring (Figure 2a), then using the Johnson−Kendall−Roberts equation[21]

$$L_{ad} = 3\pi RW \quad \text{or } W = L_{ad}/3\pi R \tag{1}$$

For symmetrical surfaces, W becomes the work of cohesion, which is related to the surface energy or surface tension, γ, by

$$\gamma = \frac{1}{2} W \tag{2}$$

Results

Characterization of the Monolayers by Contact Angle and Adhesion Measurements. The results of contact angle measurements are shown in Table 1, showing that the contact angle values of water, θ, on Au−SAM and Ag−SAM surfaces were very similar but much smaller on Ti−SAM. This suggests that the quality and coverage of the thiol monolayers on Au and Ag are much better than on Ti. The static and advancing angles,

TABLE 2: Summary of Surface Energies Obtained from the SFA Jumps In and Out

	monolayer thickness (1/2 × final separation) Å [±2 Å]	γ_{in} mJ/m^2 [eqs 3 and 4]	γ_{out} mJ/m^2 [eqs 1 and 2]
Au−SAM/Au−SAM	15	21 ± 7	41 ± 1
Ag−SAM/Au−SAM	16	20 ± 6	40 ± 1
Ti−SAM/Au−SAM	13.5	12 ± 5	57 ± 1

θ_S and θ_A, on all the surfaces were roughly the same. On the other hand, the receding angles θ_R were generally lower than the advancing angles. This "contact angle hysteresis" was largest for the Ti−SAM surface. These results indicate that the monolayers were fairly robust, but some reordering or rearrangement of the surfactant chains (and possibly headgroups) on the surfaces can take place, particularly for the Ti−SAMs. Ti rapidly forms a natural oxide layer on that surface, which competes with and thereby reduces the coverage of the surfaces by the thiol sulfur headgroups. The easier ability of the monolayers to reorder on Ti is most likely due to the lower coverage (lower surface density) of the surfactant molecules in the Ti−SAMs.

During the SFA experiments, the van der Waals and adhesion forces between the various combinations of metal−monolayer surfaces were also measured. Such measurements are useful for establishing the smoothness and cleanliness of the surfaces (by comparing the results with thermodynamic values) and also for comparing with the friction forces.

When two monolayer-coated Au surfaces were brought together in dry air, no forces were experienced until the surfaces came within about 42 Å from each other. Then, the surfaces jumped into an adhesive contact to a hard-wall distance of $D \approx 30$ Å from mica−mica contact, corresponding to two monolayers. If we assume that the jump-into contact is due to van der Waals forces between the surfaces, we can estimate the Hamaker constant, A, for the cross-cylinder geometry from[22]

$$A = \frac{3KD^3}{R} = (4.3 \pm 1.3) \times 10^{-20}\ \text{J} \qquad (3)$$

where D = jump-in distance, K = spring constant, and R = cylinder radius. From this, one can obtain the surface energy γ from the Hamaker constant using the following equation[22]

$$\gamma = \frac{A}{24\pi D_0^{\,2}} = 21 \pm 7\ \text{mJ/m}^2 \qquad (4)$$

where D_0 is the cutoff distance, typically 0.165 nm. This value is in agreement with the thermodynamic surface energy (∼25 mJ/m^2) of a typical hydrocarbon surface.

On separating the monolayer surfaces, they jump out due to their adhesion force F_{ad} from which the work of adhesion, W, and corresponding surface energy, γ, can be calculated using eqs 1 and 2. For the Au−SAMs, the value obtained was 40 mJ/m^2, about twice the thermodynamic value. Table 2 summarizes the surface energies obtained from the SFA jump-in and jump-out measurements on the three SAMs studied. The second column also gives the thicknesses of the three monolayers, where we may note that the lowest value was obtained for the Ti−SAM, consistent with the lower coverage of the SAM on Ti.

The higher adhesion values measured for all the SAMs from the jump-out distances is attributed to the interdigitation of their less than fully close-packed chains across the contacting interface, which gives rise to a higher adhesion force,[23,24] a greater adhesion and contact angle hysteresis (also as observed), and a higher expected friction force. The Ti−SAM had the highest jump-out adhesion, consistent with it being the least densely packed of the three monolayers.

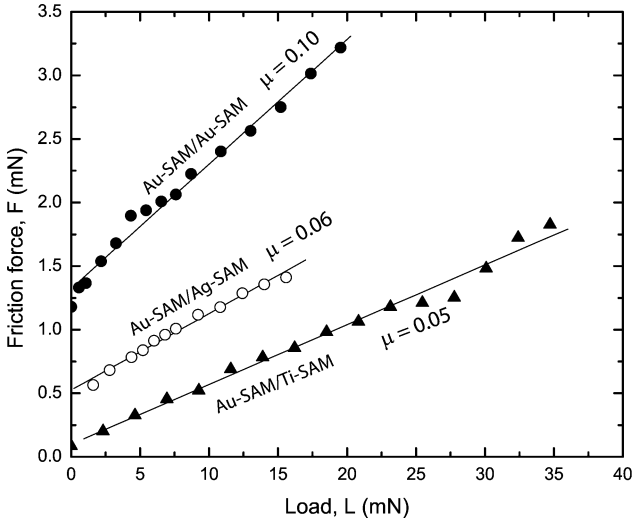

Figure 3. Friction forces as a function of load for the different systems. The friction coefficient μ is defined as $\mu = dF/dL$. The sliding velocity for all experiments was $V = 4.0$ μm/s.

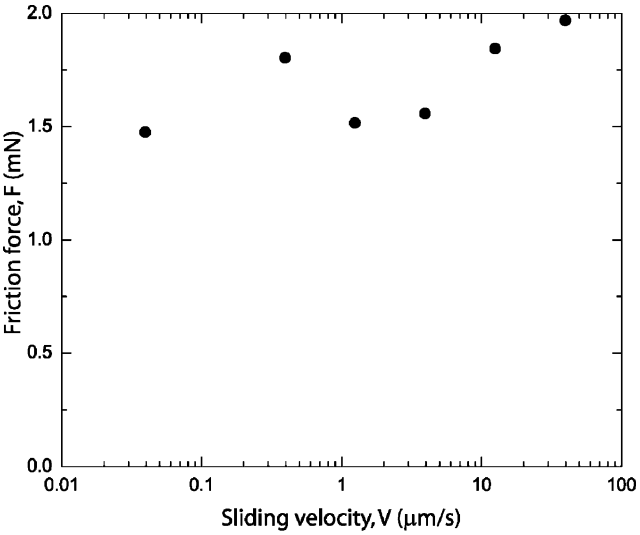

Figure 4. Friction forces F vs sliding velocity V for the Au−SAM/Au−SAM pair. The applied load, L, was ∼3 mN where the sliding was smooth (no stick−slip) at all sliding velocities V. Typical systematic errors in these friction force measurements were ±0.05 mN.

Friction Forces. The friction forces for symmetric (Au−SAM/Au−SAM) and asymmetric (Au−SAM/Ag−SAM or Au−SAM/Ti−SAM) were almost linearly proportional to the load, as shown in Figure 3. Both systems display a finite friction force at zero load due to their finite adhesion and, thus, do not obey Amontons' law $F \propto L$. However, the slope, dF/dL, was roughly constant, and this was used to define the coefficient of friction, μ. The coefficient of friction values were about 0.10 for Au−SAM/Au−SAM, 0.06 for Au−SAM/Ag−SAM, and 0.05 for Au−SAM/Ti−SAM. The highest zero-load friction and friction coefficient were observed for the symmetrical surfaces, which is generally the case in tribological systems.[25,26]

The magnitude and type of friction observed depended on the load, sliding velocity (Figure 4), sliding distance, sliding time, and the previous history, making it difficult to fully characterize or parametrize the full triboelectrification behavior.

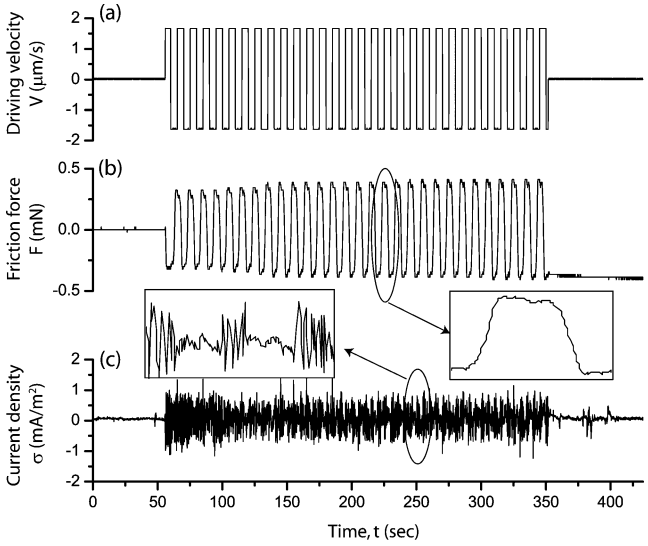

Figure 5. Back and forth sliding of a Ti−SAM surface (upper surface in Figure 2b) across a Au−SAM surface (lower surface in Figure 2b) at a low pressure of 1.4 MPa (load = 7 mN). Contact diameter = 80 μm; (a) back and forth driving velocity of 1.7 μm/s; shearing distances (before reversal) = 8.5 μm; actual sliding distance ≅ 7 μm; (b) measured friction forces; (c) measured current before (left), during (middle section), and after shearing (right).

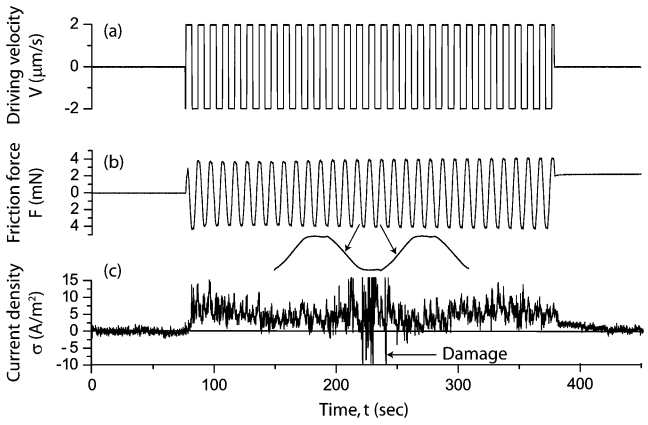

Figure 6. Same as Figure 5 but at a higher applied pressure of 6 MPa (load = 170 mN). Other experimental parameters were as follows: contact diameter = 190 μm; shearing distances (before reversal) = 10 μm; actual sliding distance ≅ 4 μm. (a) Driving velocity = 1.8 μm/s. (b) A higher friction force by a factor of ∼8. (c) A much higher time-averaged current and fluctuation than in Figure 5c, as reflected in the different current scale here. When damage occurred, the current transiently increased to a very high value (well off scale) but quickly returned to its previous steady-state values *even when passing over the same contact point*, indicative of the ability of damaged Ti−SAMs to heal.

In addition, we observed several types of friction, including smooth sliding, stick−slip sliding, and complete sticking during these experiments. Smooth sliding was the most prevalent (cf. Figures 5−8). However, certain unambiguous correlations—some quantitative, other qualitative (trends)—could be made between certain tribological parameters and the charge-transfer processes.

Triboelectrification during Sliding. We start by describing the triboelectric effects observed with the two metals that had the largest structural differences, Au and Ti. Figure 5 shows typical current density versus time traces recorded between Au−SAM and Ti−SAM at low pressures. No fluctuations were observed under static conditions (t < 55 s), but large fluctuations were observed during sliding.

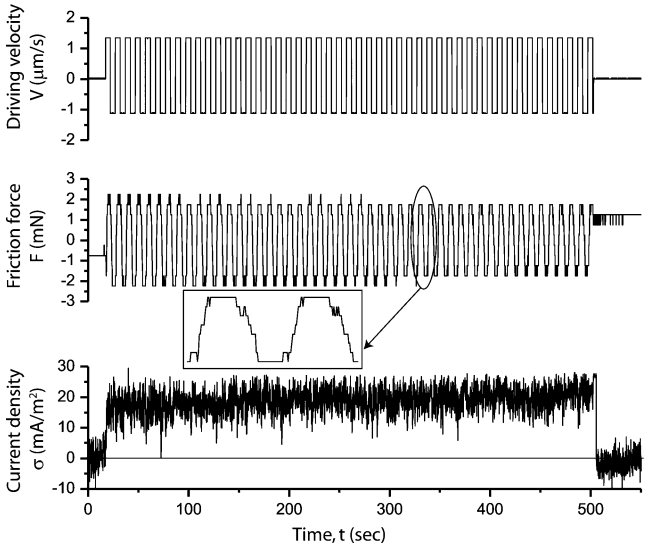

Figure 7. Same as Figure 5 but for a Ag−SAM surface sliding across a Au−SAM surface at a high applied pressure of 2.6 MPa (load = 25 mN). Other experimental parameters: contact diameter = 110 μm, sliding distance (before reversal) = 7 μm, actual sliding distance = 5 μm, and driving velocity = 1.4 μm/s. In this system under these conditions, electrons were transferred from Ag to Au.

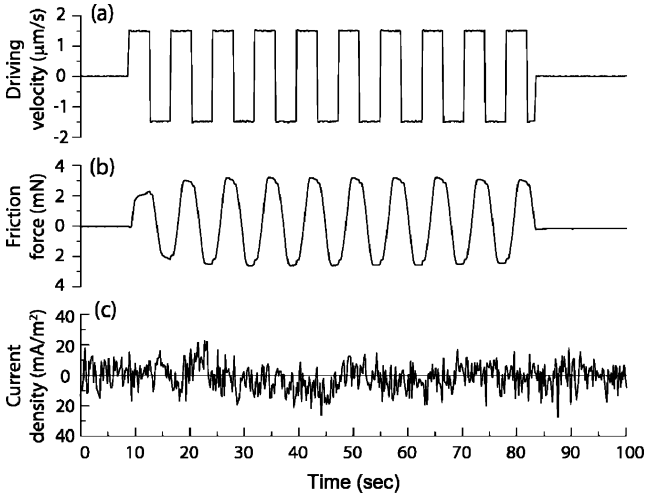

Figure 8. Same as Figures 6 and 7 but with two Au−SAM surfaces sliding across each other at a high applied pressure of ∼5 MPa (load, L = 22 mN). Other experimental parameters: contact diameter = 75 μm, sliding distances (before reversal) = 8 μm, actual sliding distance = ∼6 μm, and driving velocity = 1.5 μm/s.

Interestingly, the time-averaged, i.e., steady-state, current density during sliding was zero *within our measuring accuracy*, and certainly much smaller than the fluctuations in the current (Figure 5c). During sliding, the fluctuations were typically 0.3−0.9 mA/m^2 peak-to-peak, equivalent to $1-3 \times 10^{-3}$ e$^-$/s per hexanedecanethiol molecule. On stopping the sliding, at t = 350 s, the fluctuations decayed slowly and, at t = 400 s, disappeared completely.

At higher pressures, the friction increases proportionately, as expected, but the charge-transfer behavior changes dramatically, both quantitatively and qualitatively (Figures 6 and 7). Both the time-averaged current density as well as the amplitude of the fluctuations are *orders of magnitude* larger than at low pressures (compare 0.5 mA/m^2 or $\sim 10^{-3}$ e$^-$/s in Figure 5 to ∼10 A/m^2 or ∼12 e$^-$/s per thiol−metal complex in Figure 6). To put the latter figure of 12 e$^-$/s per $C_{16}S$ molecule into perspective, at the shearing speed of 1.8 μm/s, assuming each molecule to occupy 0.25 nm^2 (0.5 nm × 0.5 nm), the measured

current corresponds to 1 electronic charge being transferred across the gap every 300th pass of 1 molecule across the other molecules; i.e., on average, 1 in 300 molecule−molecule "collisions" leads to a charge being transferred.

On changing the top (shearing) metal surface from Ti to Ag, there was a decrease in the average current for similar pressures. Aside from these quantitative changes, there was little difference in the overall qualitative behavior of the two systems. Figure 7 shows typical current density versus time traces recorded between Au−SAM and Ag−SAM at intermediate pressures: the net charge transfer during shearing is no longer zero, and the fluctuations during sliding are larger than at static conditions.

When two identical Au−SAM surfaces were sheared against each other, the triboelectrification behavior was quite different from that occurring between the dissimilar surfaces described above: there was no measurable triboelectrification at any pressure (Figure 8).

With increasing load, the friction force also increased, and the surfaces remained "stuck" for a longer time before sliding after the motor drive was actuated. In some cases, if the distance moved by the motor drive before reversing was small, the surfaces remained stuck at all stages of the back-and-forth motion of the drive. When this occurred (see also inset in Figure 5c), the current density between the surfaces was the same as under totally static conditions (even at the moment the shear stress was abruptly applied). This shows that the measured current and especially the fluctuations are not due to electrical "noise" generated by the electrically motorized slider.

As in some previous studies on transient effects in friction,[27] it was found that the sliding *distance* is more important for attaining steady-state sliding conditions than the sliding *time*, i.e., the total distance sheared appears to be the "characteristic parameter" that determines the transition to the steady-state conditions rather than the shearing time. We found that, once the sliding distance is greater than the contact diameter (before reversing the sliding direction), the net charge transferred at high pressure was almost directly proportional to the sliding distance irrespective of the *sliding velocity* (in the range 0.2−2.0 μm/s). [Note: The friction force varied roughly logarithmically with the sliding velocity (Figure 4) and did not change much for sliding speeds between 0.2 and 2.0 μm/s.]

Figure 9 shows the results of "stop−start" friction experiments, where steady-state shearing is stopped for a certain stopping time t_s, then resumed at the same velocity. By monitoring the friction (and/or other measurable parameters) before and after stopping, and again after restarting, one can obtain important information about the relaxation processes in the system.[28] Figure 9 shows the steady growth of the friction spike upon recommencement of sliding as the stopping time t_s is increased. The friction spike (stiction) was proportional to log t_s for small stopping times and then plateaued at larger stopping times. Increasing the normal load makes the system take a longer time to reach the plateau, suggesting that the relaxation of the hexadecanethiol molecules is hindered when the applied load is larger.

After prolonged sliding, the SAMs and underlying metal surfaces sometime became damaged, as readily visualized via the interference fringes (FECO). Damage was invariably accompanied by very large current fluctuations (cf. Figure 6c), presumably due to direct metal−metal contact; but surprisingly, the friction forces did not change in any dramatic way both during and after damage (cf. Figure 6b and c), presumably because the damage was highly localized.

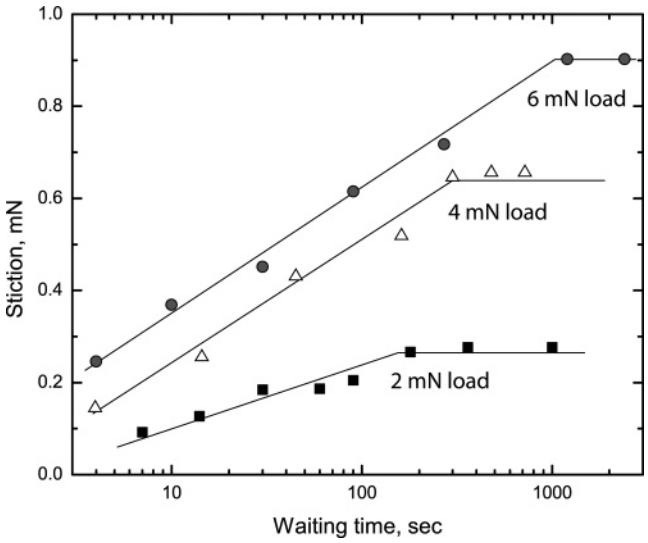

Figure 9. Stop−start friction experiments were carried out with symmetrical SAM-coated Au surfaces at various loads but the same sliding speed of $V = 4.0$ mm/s. These experiments used a piezoelectric drive rather than a mechanized motor to eliminate the mechanical motor lag time on stopping and restarting. In each case, the friction spike increased with the stopping time, t_s, as well as at increasing loads, L.

Discussion

The overall and fine details of the results give revealing insights into charge transfer and exchange between moving surfaces, which appears to be a very complex process: First, the magnitudes of both the mean current and fluctuations increase as the load, pressure, and friction forces increase; however, the former increase much more sharply than the latter. Second, the occurrence of large fluctuations (in time) is an unexpected feature of the results. Third, the organic monolayers appear to play a more active role than simply adding a nonconducting layer between the surfaces. Thus, as in the case of the friction forces that require a certain shearing distance and time to reach steady-state conditions,[48] so did the current and fluctuations, showing that the state (ordering, orientation) of the molecules in the monolayers play a key role.

Before proceeding with an overall critique of our results, one should remember that, due to geometry, there is always an asymmetry in the system even for two identical or initially symmetrical surfaces, for as soon as one surface starts to slide across the other in the common geometry shown in Figure 2b, asymmetry sets in and continues to build up.[27] This is because, while the same region of the top surface is always in contact with the lower surface, the same region of the lower surface is not always in contact with the top surface. Referring to Figure 2b, one can readily see that, regardless of which surface is actually moved relative to the laboratory frame, the motion of the two surfaces relative to each other remains asymmetric. Thus, changes occurring to the top surface, such as wear or shear-induced reordering of the atoms or molecules at this surface, are different from those at the lower surface where the molecules are continuously coming into and out of contact with those of the upper surface as it passes across the lower surface. In contrast, the molecules of the upper surface are subject to a continual shear-induced reordering with no chance to "relax" back to their unstressed state, which for surfactant monolayers can take a long time.[29]

This shear-induced asymmetry appears to contribute to the triboelectrification. It should also be noted that the two monolayers are different right from the start, since each is

attached to a different metal surface (except in the Au−SAM/Au−SAM, system where the triboelectrical effects were minimal). In addition, we stress once again that, in some of the systems studied, in particular, the high-load systems of Figures 7 and 8, the fluctuations, which are similar under static and dynamic conditions, are partly due to instrumental requirements of applying a burden voltage across the gap in order to measure the charge transfer. The amount of fluctuations generated by a burden voltage of 200 μV depends on the experimental parameters such as the pressure, sliding velocity, surfaces used, and, in turn, the monolayers' resistance (Figures 5−8). It is also important to stress that there was no charge accumulation on any surface even at high, loads since one of the surfaces was connected to ground: as soon as the two surfaces are connected through the low-resistance picoammeter, electrons flow from the surface with the lower work function to the other until the Fermi level potentials are the same. This causes the surfaces to become electrically charged, and thereby leads to the development of an electric field between them. It is also important note that, since the burden voltage of 200 μV is negligible compared to the difference in the work functions, the surface charges are mainly determined by the work functions. Thus, the triboelectrification in our experiments can be simply understood as follows: during a shearing cycle, some portion of the (tribo)-mechanical or kinetic energy supplied to the surfaces causes electrons (or charges) to move between the two shearing surfaces, which in turn causes electrons to travel around the closed external loop of the picoammeter linking the two surfaces.[50]

On the basis of the present and past tribological experience with monolayers and the present charge transfer results, we considered the following mechanisms for the charge transfer: (i) The SAM molecules pack differently on the different surfaces, for example, more tightly on Ag than on Au. The hydrocarbon chains on Au are therefore more likely to be tilted or amorphous.[30] (ii) It is well-known that Ti is chemically more reactive than Ag or Au and has a thicker natural oxide layer. The formation of an oxide layer influences the thiol assembly and, in turn, the resulting tribological properties,[31] for example, lower damage resistance. (iii) SAMs are generally imperfect structures, possessing defects, domains, and amorphous regions even under static conditions,[32] while during sliding, their chains continually entangle and disentangle across the shearing interface. During sliding, the chains in the top monolayer experience a *continuous* shear force, while those in the bottom monolayer experience a *transient* force as they come into and out of the contact region. (iv) Inside the contact area, chain reordering depends on the *distance* sheared, while outside the contact area, the lower surface molecules slowly relax back to their unconfined, unsheared state (see "Near back" region in Figure 2b) which depends on the *time*. All of these effects depend on the contact area, load (pressure), shearing velocity and time, and the characteristic relaxation times and distances of the SAMs, both when confined and unconfined. These effects in turn determine both the friction forces and triboelectrification.

Regarding the change in the coefficient of friction with respect to the metal substrate, it is known that when a bare metal surface is sheared against a monolayer-coated surface the friction coefficient is much smaller than that when two monolayer-coated surfaces are sheared against each other.[33] This is because there is no interdigitation and entanglement between a bare metal surface and the hydrocarbon chains of the adsorbed surfactant molecules. On the other hand, there are entanglements and interdigitations between two contacting and shearing monolayers, leading to the higher friction forces.[34,35] In addition, the friction coefficient is typically higher for symmetrical than asymmetrical surfaces because of the higher likelihood of interdigitation (mixing of similar chains) in the former case.[25,26,49] The very low zero-load friction force for the Ti−SAM/Au−SAM system is likely due to the fluidity of the low-density Ti−SAM that therefore exhibits a more viscous friction force and small "adhesion-controlled" friction. The coefficient of friction for the Ti−SAM/Au−SAM system was the smallest measured, most likely due to a combination of the above effects.

As mentioned in the Introduction, various mechanisms have been proposed to explain how charges are produced and transported across the monolayers. We first consider the charge generation mechanisms in light of our results.

(i) Different shear-induced local (shear) stresses on monolayers and materials are expected to influence both static charge transfer and triboelectrification.[14,36] Since there was no measurable triboelectrification as the shear stress was increased from zero to a maximum value that was still below the stress needed to initiate motion (resulting in pure sticking friction), we can conclude that the effect of a pure stress and strain on charge transfer between the SAMs is negligible.

(ii) Bowles[13] proposed that a temperature difference between a moving and stationary surfaces would induce a Seebeck−Thompson voltage difference resulting in charge transfer. During shearing, both symmetric (Au−SAM/Au−SAM) and asymmetric surfaces (Au−SAM/Ag−SAM or Au−SAM/Ti−SAM) would produce a temperature difference between moving and stationary surfaces. If the charge transfer were a consequence of this effect, both the symmetric and asymmetric surfaces would produce a finite net charge transfer during shearing. However, our results showed that there is a net charge transfer for asymmetric surfaces and no charge transfer for symmetric surfaces at high pressures. In addition, our results show that sliding velocity does not have any significant influence on charge transfer. However, it is known that sliding velocity influences frictional heating. Thus, we conclude that friction-induced temperature differences are not responsible for triboelectrification.

(iii) Another possible mechanism for the triboelectrification is material transfer.[37] Our result showed that, at high pressures, there is a finite net charge transfer for the asymmetric surfaces and no net charge transfer for the symmetric surfaces. However, material transfer should take place irrespective of the type of surfaces used. Thus, if the material transfer is the main source of triboelectrification, then both the symmetrical and asymmetrical surfaces should have produced a finite charge transfer. In addition, the fluctuations in the current density were too reproducible to be created just by material transfer. It is worth recalling that the triboelectrification observed when the surfaces became locally damaged (Figure 6c) was significantly larger than the triboelectrification in the absence of damage. Thus, we can conclude that if there is material transfer, this can lead to charge transfer. However, the reverse is not necessarily true.

(iv) For our type of system, since the two metals are connected externally through the picoammeter, the Fermi levels of the two metals are already equal before the metals are brought into contact when electrons are expected to flow from the surface with the lower work function to the other. This causes the two conducting surfaces to be electrically charged, with the development of an electric field across the gap. As the surfaces slide past each other, local (nanoscale) changes/fluctuations in the thickness, including local charge displacements as a function of position, due to roughness and imperfections, generate a

tribocurrent. In addition, since the structure of the monolayers, especially the upper one in Figure 2b, changes as a function of shearing, this could also generate tribocurrents. A combination of these effects could explain the existence of the fluctuations in the tribocurrent.

(v) The final mechanism we consider involves the formation of electron−hole (e−h) pairs. It is known that an electron−hole population can be created by various energy dissipation processes, e.g., optical pulses, chemical reactions, adsorption, and thermal ionization;[38−42] frictional energy dissipation can also create electron−hole pairs. The system eventually relaxes back via the recombination of the electron and holes through the external circuit. The direction of e−h flow is determined by the direction of the quiescent electric field. This field most probably determines the directionality of the tribocurrent. One may expect that it is easier to produce electron−hole pairs from oxides than metals, because oxides have more defects. This effect could account for higher tribocurrent observed with the Ti−SAMs because of the thicker oxide layer on Ti. The correlation of the higher triboelectrification with the higher friction would then be indirect—both being a result of the Ti−SAM structure, rather than the one being the cause of the other, as discussed further below.

On the basis of the above mechanisms, we now discuss how the charge is transported through the monolayers and how the frictional parameters are correlated with the triboelectrification.

To measure a finite current through the picoammeter, charges first have to flow from one surface to the other across the two monolayers (see ref 50). For example, after electrons or an e−h pair are created at a surface, one of the species has to travel to the other surface to generate a measurable current through the external circuit. The transfer across the monolayers is probably achieved via electron tunneling through transient low-resistance or low-dielectric-constant nanoscale defects.[43] Electron tunneling is known to decay sharply and exponentially with the metal/metal separation,[44] which is the likely reason for why the measured tribocurrent is very sensitive to the applied load (pressure) which changes the mean (and probably also local, transient) surface separations. A similar load dependence was observed by Son et al.,[14] where an external voltage was applied to investigate charge transfer through an alkanethiol SAM. The results showed that charge transfer through the monolayer is only feasible when there is good contact between the tip and film surface, which was achieved by applying a high compressive stress. Similarly, Barrena et al.[45] showed that thiol chains in Au(111)−SAMs can form tilted phases where the monolayer thickness can decrease by a few ångstroms as the applied load or stress is increased. It is also possible that the intrinsic conduction of tilted or ordered chains is quite different from amorphous chains, and interdigitated chains may also differ from noninterdigitated chains.

In light of all of these findings by us and others, we can state that the strong dependence of the tribocurrent on the load is probably a manifestation of the high sensitivity of electron tunneling to small changes in the monolayers' thickness, structure and degree of interdigitation.

Higher tribocurrents were generally associated with higher friction forces, both of which were particularly sensitive to the load and type of SAM. More specifically, the friction forces were not as sensitive to the load as the tribocurrents. Concerning the different SAMs, the net triboelectrification of Au−SAM on Ti−SAM was larger than for Au−SAM on Ag−SAM. The former pair has the larger structural difference and thicker oxide layer. As already described, SAMs on Ti are thinner, less densely packed, and are likely to have more point defects. Electron−hole pairs should therefore travel more easily through Ti−SAMs, and the thinner monolayers should facilitate electron tunneling, further increasing the measured tribocurrent.

The above mechanisms, especially (iv) and (v), apply principally to asymmetric monolayers. For symmetric monolayers when these are connected through the picoammeter, no electric field develops across the surfaces. Thus, even if electron−hole pairs form, the liberated charges will not be driven in any particular direction. Furthermore, because there is no electric field or charge motion between the surfaces, any change in surface separation or local dielectric constant does not produce any current. For symmetric monolayers, we therefore expect little or no tribocurrent, and none was observed. It is apparent that any possible shear-induced asymmetry generated in the (initially) symmetric monolayers, discussed earlier, was negligible, thereby also attesting to the robustness of the monolayers during prolonged sliding.

In light of our results and those of others,[7−15] the picture that emerges is that triboelectrification occurs due to a combination of two effects: (a) frictional energy dissipation-induced charge displacements or electron−hole formation, and (b) changes in the electric field between two surfaces due to molecular-level roughness and local dielectric constant changes. The latter effect is responsible for the existence of fluctuations, the former for the net (mean) current. This would explain (i) the high sensitivity of the current to the applied pressure, (ii) the large fluctuations when two surfaces slide past each other, (iii) the unidirectionality of the net current for asymmetric surfaces, and (iv) the lack of fluctuations and net charge transfer when two symmetric surfaces are sheared against each another.

Conclusions

We show that, when two asymmetric SAM-coated metal surfaces are sheared against each other, there are large current fluctuations, which increase with the applied load (pressure) and friction. In addition, there is no net measurable charge transfer at low pressures and a finite net charge transfer at high pressures. These effects are larger between the Ti−SAM and Au−SAM pair than between the Ag−SAM and Au−SAM pair where the Ti has a thicker layer of native oxide. On the other hand, when two symmetric surfaces are sheared against one another, there is no current fluctuation and no net charge transfer at both low and high pressures. The load, sliding distance, contact area, and previous history play a significant role in triboelectrification (and the friction forces). Interestingly, triboelectrification was found to be much more sensitive to some of these parameters than was the friction force. We propose that tribocurrents are induced by frictional energy dissipation that creates electron−hole pairs which then tunnel across the gap and that charge fluctuations are induced by local, transient changes in the electric field between two shearing surfaces due to the molecular-level roughness and local dielectric constant variations.

Acknowledgment. This work was supported by ONR grant no. N00014-05-1-0540. We also thank one of the anonymous reviewers for enlightening us on how to interpret our results.

References and Notes

(1) Lowell, J. Contact Electrification of Metals. *J. Phys. D: Appl. Phys.* **1975**, *8* (1), 53−63.

(2) Horn, R. G.; Smith, D. T. Contact Electrification and Adhesion between Dissimilar Materials. *Science* **1992**, *256* (5055), 362−364.

(3) Brennan, W. J.; Lowell, J.; O'Neill, M. C.; Wilson, M. P. W. Contact Electrification − the Charge Penetration Depth. *J. Phys. D: Appl. Phys.* **1992**, *25* (10), 1513−1517.

(4) Derjaguin, B. V.; Smilga, V. P. Electrostatic component of the rolling friction force moment. *Prog. Surf. Sci.* **1994**, *45* (1−4), 296−307.

(5) Derjaguin, B. V.; Smilga, V. P. The effect of the double electric layer on rolling friction (the electrical component of rolling friction). *Prog. Surf. Sci.* **1994**, *45* (1−4), 108−118.

(6) Fischer, T. E. Tribochemistry. *Annu. Rev. Mater. Sci.* **1988**, *18*, 303−323.

(7) Budakian, R.; Putterman, S. J. Correlation between charge transfer and stick-slip friction at a metal−insulator interface. *Phys. Rev. Lett.* **2000**, *85* (5), 1000−1003.

(8) Greason, W. D.; Oltean, I. M.; Kucerovsky, Z.; Ieta, A. C. Triboelectric charging between polytetrafluoroethylene and metals. *IEEE Trans. Ind. Appl.* **2004**, *40* (2), 442−450.

(9) Nakayama, K. Tribocharging and friction in insulators in ambient air. *Wear* **1996**, *194* (1−2), 185−189.

(10) Ohara, K.; Uchiyama, S. Frictional Electrification of Fatty-Acid Lb Films of Which the Uppermost Layer Was Deposited on Y-Type Films by the Horizontal Lifting Method. *J. Phys. D: Appl. Phys.* **1992**, *25* (1), 94−99.

(11) Guerret-Piecourt, C.; Bec, S.; Treheux, D. Electrical charges and tribology of insulating materials. *C. R. Acad. Sci., Ser. IV: Phys. Astrophys.* **2001**, *2* (5), 761−774.

(12) Davies, D. K. Charge Generation on Dielectric Surfaces. *J. Phys. D: Appl. Phys.* **1969**, *2*, (11), 1533-&.

(13) Bowles, A. H. Effect of a Thermal Gradient Upon Charge Separation between Similar Polyethylene Surfaces. *Proc. Phys. Soc. London* **1961**, *78* (504), 958 ff.

(14) Son, K. A.; Kim, H. I.; Houston, J. E. Role of stress on charge transfer through self-assembled alkanethiol monolayers on Au. *Phys. Rev. Lett.* **2001**, *86* (23), 5357−5360.

(15) Guerret-Piecourt, C.; Bec, S.; Segault, F.; Juve, D.; Treheux, D.; Tonck, A. Adhesion forces due to nano-triboelectrification between similar materials. *Eur. Phys. J.: Appl. Phys.* **2004**, *28* (1), 65−72.

(16) Potter, H. C.; Blakely, J. M. Leed, Auger-Spectroscopy, and Contact Potential Studies of Copper−Gold Alloy Single-Crystal Surfaces. *J. Vac. Sci. Technol.* **1975**, *12* (2), 635−642.

(17) Dweydari, A. W.; Mee, C. H. B. Oxygen Adsorption on (111) Face of Silver. *Phys. Status Solidi A* **1973**, *17* (1), 247−250.

(18) Eastman, D. E. Photoelectric Work Functions of Transition, Rare-Earth, and Noble Metals. *Phys. Rev. B* **1970**, *2* (1), 1 ff.

(19) Luengo, G.; Schmitt, F. J.; Hill, R.; Israelachvili, J. Thin film rheology and tribology of confined polymer melts: Contrasts with bulk properties. *Macromolecules* **1997**, *30* (8), 2482−2494.

(20) Israelachvili, J. N. Thin film studies using multiple-beam interferometry. *J. Colloid Interface Sci.* **1973**, *44* (2), 259−72.

(21) Johnson, K. L.; Kendall, K.; Roberts, A. D. Surface Energy and Contact of Elastic Solids. *Proc. R. Soc. London, Ser. A* **1971**, *324* (1558), 301 ff.

(22) Israelachvili, J. *Intermolecular and Surface Force*. 2nd ed.; Acedemic Press: San Diego, 1992.

(23) Chen, Y. L.; Helm, C. A.; Israelachvili, J. N. Molecular Mechanisms Associated with Adhesion and Contact-Angle Hysteresis of Monolayer Surfaces. *J. Phys. Chem.* **1991**, *95* (26), 10736−10747.

(24) Chen, Y. L.; Xu, Z. H.; Israelachvili, J. Structure and Interactions of Surfactant-Covered Surfaces in Nonaqueous (Oil Surfactant Water) Media. *Langmuir* **1992**, *8* (12), 2966−2975.

(25) Heuberger, M.; Luengo, G.; Israelachvili, J. N. Tribology of shearing polymer surfaces. 1. Mica sliding on polymer (PnBMA). *J. Phys. Chem. B* **1999**, *103* (46), 10127−10135.

(26) Luengo, G.; Heuberger, M.; Israelachvili, J., Tribology of shearing polymer surfaces. 2. Polymer (PnBMA) sliding on mica. *J. Phys. Chem. B* **2000**, *104* (33), 7944−7950.

(27) Drummond, C.; Israelachvili, J. Dynamic behavior of confined branched hydrocarbon lubricant fluids under shear. *Macromolecules* **2000**, *33* (13), 4910−4920.

(28) Persson, B. N. J. *Sliding friction: physical principles and applications*. 2nd ed.; Springer: Berlin, 2000; pp xi, 515.

(29) Grossiord, C.; Martin, J. M.; Varlot, K.; Vacher, B.; Le Mogne, T.; Yamada, Y. Tribochemical interactions between Zndtp, Modtc and calcium borate. *Tribol. Lett.* **2000**, *8* (4), 203-212.

(30) Ulman, A. Formation and structure of self-assembled monolayers. *Chem. Rev.* **1996**, *96* (4), 1533−1554.

(31) Sung, I. H.; Yang, J. C.; Kim, D. E.; Shin, B. S. Micro/nano-tribological characteristics of self-assembled monolayer and its application in nano-structure fabrication. *Wear* **2003**, *255*, 808−818.

(32) Komura, T.; Yamaguchi, T.; Shimatani, H.; Okushio, R. Interfacial charge-transfer resistance at ionizable thiol monolayer-modified gold electrodes as studied by impedance spectroscopy. *Electrochim. Acta* **2004**, *49* (4), 597−606.

(33) Qian, L. M.; Tian, F.; Xiao, X. D. Tribological properties of self-assembled monolayers and their substrates under various humid environments. *Tribol. Lett.* **2003**, *15* (3), 169−176.

(34) Ruths, M. Boundary friction of aromatic self-assembled monolayers: Comparison of systems with one or both sliding surfaces covered with a thiol monolayer. *Langmuir* **2003**, *19* (17), 6788−6795.

(35) Ruths, M. Friction of mixed and single-component aromatic monolayers in contacts of different adhesive strength. *J. Phys. Chem. B* **2006**, *110* (5), 2209−2218.

(36) Shaw, P.; Hanstock, R. F. *Proc. R. Soc.* **1930**, *128*, 474.

(37) Lowell, J.; Roseinnes, A. C. Contact Electrification. *Adv. Phys.* **1980**, *29* (6), 947−1023.

(38) Haight, R. Electron dynamics at semiconductor surfaces and interfaces. *Chem. Phys.* **1996**, *205* (1−2), 231−244.

(39) Shah, J.; Dayem, A. H. Formation of Electron−Hole Liquid in Optically-Excited Si − Results of Fast Time-Resolved Spectroscopy. *Phys. Rev. Lett.* **1976**, *37* (13), 861−864.

(40) Nienhaus, H.; Gergen, B.; Weinberg, W. H.; McFarland, E. W. Detection of chemically induced hot charge carriers with ultrathin metal film Schottky contacts. *Surf. Sci.* **2002**, *514* (1−3), 172−181.

(41) Kroger, J.; Limot, L.; Jensen, H.; Berndt, R.; Crampin, S.; Pehlke, E. Surface state electron dynamics of clean and adsorbate-covered metal surfaces studied with the scanning tunnelling microscope. *Prog. Surf. Sci.* **2005**, *80* (1−2), 26−48.

(42) Witte, G.; Weiss, K.; Jakob, P.; Braun, J.; Kostov, K. L.; Woll, C. Damping of molecular motion on a solid substrate: Evidence for electron−hole pair creation. *Phys. Rev. Lett.* **1998**, *80* (1), 121−124.

(43) Nahir, T. M.; Bowden, E. F. Impedance Spectroscopy of Electroinactive Thiolate Films Adsorbed on Gold. *Electrochim. Acta* **1994**, *39* (16), 2347−2352.

(44) Weiss, P. S.; Bumm, L. A.; Dunbar, T. D.; Burgin, T. P.; Tour, J. M.; Allara, D. L. Probing electronic properties of conjugated and saturated molecules in self-assembled monolayers. *Mol. Electron.: Sci. Technol.* **1998**, *852*, 145−168.

(45) Barrena, E.; Ocal, C.; Salmeron, M. Structure and stability of tilted-chain phases of alkanethiols on Au(111). *J. Chem. Phys.* **2001**, *114* (9), 4210−4214.

(46) When comparing the results of different experiments, the highest load does not necessarily correspond to the highest pressure because of the different thicknesses of the glue layers used to support the mica substrates. Different glue layer thicknesses give rise to different stiffnesses of the mica "backing" and, therefore, different contact areas for a given load.

(47) It is important to mention that, since these surfaces contained a light-absorbing layer of thin metal, the sharpness and intensity of the FECO were reduced. This caused a reduction in accuracy (or resolution) of measuring surface separations to ±3−4 Å (±1.5−2.0 Å per monolayer when one is present on each surface) instead of the typical resolution of ±1 Å.

(48) These different distances and times reflect the different molecular processes associated with the "forced adaptation" and "natural relaxation" of tribological systems.

(49) Different surfaces have a finite interfacial energy which inhibits mixing.

(50) A common physics problem is to show that, when a charge Q located within the nonconducting gap between two capacitor plates (conducting electrode surfaces) moves a distance d normal to the surfaces, the charge flowing through an external wire connecting the two electrodes is Qd/D. This result is independent of any fixed voltage applied across the electrode surfaces.